Comparative Medicine
Copyright 2023
by the American Association for Laboratory Animal Science

Vol 73, No 5
October 2023
Pages 357–372

Original Research

Evaluation of Selected Markers in Kidneys of Cynomolgus Monkey (*Macaca fascicularis*) with Induced Diabetes during Renal Ischemia-reperfusion Injury

Tae M Kim,[1,2,*] Kyo W Lee,[3] Hong D Kim,[2] Sung O Hong,[2] Hye J Cho,[1] Je H Yang,[4] Sung J Kim,[5] and Jae B Park[3,*]

We previously reported that induced type 1 diabetes mellitus (DM) increases the susceptibility of acute kidney injury induced by ischemia-reperfusion injury (IRI) in cynomolgus monkeys. In this follow-up study, we compared the expression of selected markers in the renal tissues of monkeys subjected to bilateral renal IRI with and without diabetes. All tissues were obtained from the original study. Renal biopsies were obtained before and 24 and 48 h after ischemia and were examined for expression of KI-67 (tubular proliferation), Na^+/K^+ ATPase (sodium-potassium pump), TNF-α (tumor necrosis factor-α, inflammation), CD31 (microvessels), CD3 (T-cells), 2 fibrotic markers (fibroblast specific protein-1, FSP-1; α-smooth muscle actin, α-SMA), and cleaved caspase 3 (apoptosis). Generally, the expression of these markers differed in monkeys with and without DM. As compared with non-DM monkeys, DM monkeys had more cells that expressed KI-67 during progression of acute kidney injury (AKI). Na^+/K^+ ATPase expression was clearly present at baseline in the basolateral tubular areas only in the non-DM monkeys. At 48 h, its expression in the basolateral area was not visible in DM monkeys, but was still present in intercellular junctions of non-DM monkeys. The expression of TNF-α was higher in DM before and 48 h after ischemia. Before and 24 h after ischemia, the number of CD31-positive capillaries was not different between 2 groups, although more collapsed vessels were found at in DM at 24 h. At 48 h, the number of capillaries was less in DM compared with those from non-DM animals. DM monkeys had more interstitial CD3-positive cells than did non-DM monkeys at 24 and 48 h after ischemia. Finally, FSP-1-stained cells were more abundant in DM than non-DM at 24 and 48 h. Our results show that DM aggravates the recovery of renal ischemia/reperfusion injury by affecting tubular proliferation, capillary density, T cell infiltration and by altering protein and mRNA expression of various genes involved in ion channel, inflammation, and fibrotic change. The results from this observational study demonstrate that DM aggravates the recovery of renal ischemia/reperfusion injury by affecting multiple events including tubular necrosis, proliferation, function, inflammation and by inducing capillary rarefaction in cynomolgus monkeys.

Abbreviations and Acronyms: α-SMA, alpha-smooth muscle actin; AKI, acute kidney injury; DM, diabetes mellitus; FSP-1, fibroblast-specific protein-1; IHC, immunohistochemistry; IRI, ischemia-reperfusion injury; Na^+/K^+ ATPase, sodium/potassium adenosine triphosphatase; TNF-α, tumor necrosis factor-α

DOI: 10.30802/AALAS-CM-22-000127

Introduction

The prevalence of diabetes mellitus (DM) has risen over the last decade. DM affects approximately 422 million individuals globally according to a meta-analysis done in 2014.[54] Multiple studies have reported that DM is a major risk factor for acute kidney injury (AKI),[18,20,52] and that AKI independently increases the risk of chronic kidney disease in diabetic patients.[47] AKI is characterized by a sudden reduction in renal function caused by renotoxic drugs, sepsis, obstruction, renal hypoperfusion, and ischemia/reperfusion injury (IRI).[26] AKI is one of the main causes of chronic renal disease in DM[41] and can progress to end stage renal disease (ESRD). Rodent studies confirm that DM augments the severity of AKI.[22,39]

Most pre-clinical studies on AKI have been performed using rodents; however, the physiology and local or systemic inflammatory responses of humans and mice differ,[37,46] as do various cellular traits and molecular profiles.[31] Studies using large animal models often improve insights relevant to clinical translation.[37,48] We previously reported that in a renal IRI model using in diabetic cynomolgus monkeys (*Macaca fascicularis*),

Submitted: 08 Dec 2022. Revision requested: 26 Jan 2023. Accepted: 04 May 2023.
[1]Graduate School of International Agricultural Technology, Seoul National University, Pyeongchang, Gangwon-do 25354, South Korea, [2]Institutes of Green-Bio Science and Technology, Seoul National University, Pyeongchang, Gangwon-do 25354, South Korea, [3]Department of Surgery, Samsung Medical Center, Sungkyunkwan University School of Medicine, 81 Irwon-ro, Gangnam-gu, Seoul 06351, South Korea, [4]Laboratory Animal Research Center, Samsung Medical Center, 81 Irwon-ro, Gangnam-gu, Seoul 06351, South Korea, [5]GenNBio Inc., 80 Deurimsandan 2-ro, Cheongbuk-myeon, Pyeongtaek-si, Gyeonggi-do 17796, South Korea
**Corresponding authors. Email: jbparkmd@gmail.com and taemin21@snu.ac.kr*

DM increases susceptibility to AKI in association with a marked increase in tubular damage, including hyaline cast formation and tubular necrosis, and in serum functional and inflammatory biomarkers.[28] That initial study did not examine the expression of other marker that could further elucidate the relationship between diabetes and AKI progression induced by IRI. Comparing the expression of key markers in the kidney of monkeys undergoing AKI may contribute to better clinical translation in understanding the effect of DM on aggravated recovery of AKI.

Herein, we performed immunohistochemical and qRT-PCR analysis on the expression of selected markers that can indicate proliferation/apoptosis (KI-67 and cleaved caspase 3), electrolyte exchange pump (Na^+/K^+ ATPase), inflammation (TNF-α), vessel density (CD31), T cell presence (CD3), and fibrotic change (FSP-1, α-SMA) in kidney tissue biopsies at different time points in non-DM and DM monkeys after IRI.

Materials and Methods

Animal experiments. The tissue slides examined in this study were from the previous study.[28] Male cynomolgus monkeys (*Macaca fascicularis*) aged 5 to 6 y and weighing between 3.5 to 5 kg were used. A total of 6 animals were used (3 each for non-DM and DM). All animals originated in Cambodia. Animal procedures were conducted in accordance with the *Guide for the Care and Use of Laboratory Animal*[42] and the Animal Welfare Act[1] in the animal facility of the Primate Organ Transplantation Research Center at Genia (Sung-nam City, Korea). Study protocols were approved by the Institutional Animal Care and Use Committee of Orient Bio (ORIENT–IACUC–16317). The temperature and humidity of rooms were maintained at 23 to 25 °C and 40 to 60%, respectively. Monkeys were housed individually in cages. The light was turned on and off at 0800 and 2000, respectively. Kong toys (Primate Products, Immokalee, FL) were provided as an enrichment program. Animals received standard biscuits (Certified Primate Diet 5048, LabDiet, St. Louis, MO) and fruits twice every day. Filtered water was provided ad libitum. During the study period, monkeys were tested for tuberculosis every 6-mo using a commercial kit (SD Bioline TB Ag MPT64 RAPID, Standard Diagnostics, Yongin-si, South Korea), and all animals tested negative. Tests for herpes B virus, simian T-cell leukemia virus, simian retrovirus, simian immunodeficiency virus, measles, cynomolgus cytomegalovirus, and simian varicella virus were conducted at a diagnostic laboratory (Zoologix, Chatsworth, CA), and all gave negative results.

Induction of diabetes mellitus and postoperative care. After a 12-h fast, monkeys were injected intramuscularly with ketamine (10 mg/kg). They were then intubated with endotracheal tubes (4.0 to 4.5 Fr) and anesthetized with 3 to 5% isoflurane. After induction, anesthesia was maintained with 1% to 2% isoflurane in nitrous oxide and oxygen (2:1 ratio). Hypothermia was prevented by using heating pads, injecting warm saline, and wrapping extremities. Antibiotics (20 mg/kg cefazolin sodium, IV) were given at the time of the skin incision.

Betadine soap and 10% betadine solution were used to disinfect the skin. Through an incision in the upper midline, the omentum was exposed. To minimize postoperative adhesions, wet gauze was used to wrap the bowel. The spleen and pancreas were identified as the stomach was being retracted. Short stomach vessels and the gastrosplenic ligament were ligated and separated. The spleen and pancreas from the tail to the body were mobilized. The pancreas was transected at the level of the superior mesenteric artery and portal vein after ligation and division of the splenic artery and veins. This procedure removed almost 70% of the pancreas. Omentum was used to cover the bowel, after which the fascia and skin layers were closed with absorbable sutures, with the knots were positioned beneath the skin. Immediately after pancreatectomy, streptozotocin (60 mg/kg, Sigma, St. Louis, MO) dissolved in 10 mL of normal saline was injected through a central venous catheter (3 Fr) inserted into the internal jugular vein. Monkeys received 2 mg/kg tramadol for 3 d after surgery, with 2 to 3 injections per day. Food was provided on the day after surgery, initially dampened with water and then gradually advancing to a normal diet. All animals consumed food during the postoperative period.

Validating diabetes. Type 1 DM (T1DM) was diagnosed after the following criteria were met: (1) sustained hyperglycemia (> 250 mg/dL), (2) fasting C-peptide level less than either 0.5 ng/mL or one-third of the value at preinduction stage, and (3) the absence of stimulated C-peptide response on intravenous glucose tolerance test (IVGTT). Serum C-peptide was measured using a commercial kit (C-peptide IRMA kit; IMMUNOTECH, Beckman Coulter, Prague, Czech Republic). After a 12 h fast, monkeys received intravenous glucose (0.5 g/kg). Blood samples were drawn at 1, 3, 5, 7, 10, 15, 20, 25, 30, and 60 min after the glucose infusion. The acute C-peptide response (ACR) was calculated as the difference between mean C-peptide concentration at each time point after glucose infusion and C-peptide at baseline. To obtain the glucose disappearance rate (KG, %/min), the slope of the decline in the log-transformed value of blood glucose between 10 and 30 min was determined. Blood glucose levels were measured 3 to 4 times daily in T1DM animals. During the postoperative period, body weight measurement and physical examinations were conducted once every week. The following hematologic parameters were also monitored every week: white blood cell count (WBC) with differential count, hemoglobin (Hb), hematocrit and platelet count, aspartate aminotransferase (AST), alanine aminotransferase (ALT), alkaline phosphatase (ALP), total bilirubin, blood urea nitrogen (BUN), creatinine, albumin, globulin, inorganic phosphorus, cholesterol, triglyceride, amylase, C-reactive protein (CRP), and electrolytes (sodium, potassium, chloride, calcium).The blood glucose level was maintained (200 to 300 mg/dL) using insulin (glargine [Lantus, Sanofi-Aventis, Bridgewater, NJ] and glulisine [Apidra, Sanofi-Aventis]). The fasting glucose levels of non-DM monkeys and DM-monkeys were < 100 mg/dL and > 250 mg/dL in all cases for at least for 5 mo prior to this study.

Renal ischemia-reperfusion. The same anesthetic and preoperative preparation protocol was used as described for the partial pancreatectomy above. The abdominal cavity was entered through a midline incision. Thereafter the right colon was mobilized to expose the right renal pedicle; the left colon was mobilized to expose the left renal pedicle. Before clamping, a biopsy sample was collected using free hand techniques. An 18-gauge semiautomated needle was used for sampling (Argon Medical Devices, Plano, TX). Upon confirming the lack of bleeding, renal pedicle was clamped in a bundle with bulldog clamp for an hour and released. Upon release, the outward color changes of the kidney were observed over time. After the procedure, the abdominal wall was closed in a layer-by-layer manner. A total of three biopsy tissue, one from each time point (0, 24, and 48 h), was collected.

Ultrasound-guided renal biopsy. At 24 and 48 h after reperfusion, animals were sedated with intramuscular injection of ketamine hydrochloride (10 mg/kg).[13] Ultrasound-guided percutaneous biopsy was performed by kidney transplant surgeon who usually performs the procedure in humans. Single biopsy tissue was obtained from each animal at each time point. Biopsies from right kidneys were guided with 9 L linear

transducer and the LOGIQ E9 system (GE Healthcare, Waukesha, WI). After controlling gray-scale and Doppler-scale parameters, we assessed the kidney size, cortical echogenicity, and collecting system. The renal cortex was biopsied in the location deemed to be the most safely accessible. Biopsy cores were sampled with free hand techniques; a biopsy guider was not set on the probe. An 18-gauge semiautomated needle was used for sampling (Argon Medical Devices, Plano, TX). Manual compression was routinely used after biopsy to minimize bleeding; ultrasound was used after compression to determine if bleeding was present. When bleeding was detected, we continued manual compression of the biopsy site until bleeding had disappeared on ultrasound. The collected tissue was cut into two and used for histology/immunohistochemistry and RNA extraction.

RNA extraction, cDNA synthesis, and qRT-PCR. Total RNA was extracted from one piece of the biopsy tissue by using TRIzol (Thermo Fisher Scientific, Carlsbad, CA), following the manufacturer's instructions. cDNA was synthesized using 200 ng of total RNA using a cDNA synthesis kit (Philekorea, Daejeon, Korea), and qPCR was performed using Accupower 2× GreenStar qPCR Master Mix (Bioneer, Daejeon, Korea) in a CFX96 Touch Real-Time PCR Detection System (Bio-Rad Laboratories, Hercules, CA). The expression of each gene was normalized against MRFAP1 (Morf4 Family Associated Protein 1)[38] and relative expression was analyzed using the $2^{-\Delta\Delta Ct}$ method.[32] Primer sequences are listed in Table 1. Expression of the MRFAP1 gene (which encodes the MORF4 family-associated protein 1) was used for normalization in qPCR assays. The representative amplification plots of genes from each sample are shown in Figure 1.

Histology and immunohistochemistry. The other piece of the renal biopsy tissue was fixed in 10% neutral buffered formalin (Biosesang, Sungnam-si, Korea) for 24 h, and embedded in paraffin wax. Tissue sections (5-μm-thickness) were deparaffinized in xylene. After slides were hydrated in steps of descending concentration of ethanol from 100 to 70%, tissue was treated with an antigen retrieval buffer (citrate buffer, pH 6.0; Abcam, Cambridge, UK) according to the manufacturer's instructions. Immunostaining was performed using the UltraVision LP Detection System HRP DAB kit (Thermo Fisher Scientific, Waltham, MA) according to the instructions. All primary antibodies were incubated overnight at 4 °C. Detailed information on the primary and secondary antibodies is provided in Table 2. After DAB reaction, the slides were counterstained in Mayer's hematoxylin (4science, Korea) for 20 s at room temperature. Slides were then dehydrated in steps of ascending concentration of ethanol from 70 to 100%, embedded with resin, and covered with coverslips. Nonoverlapping images were obtained using an Olympus BX43 light microscope (magnification, ×400; Olympus Corporation, Tokyo, Japan). The biopsy conducted before ischemia was used as baseline control.

The number of positively-stained cells (KI-67, Na^+/K^+ ATPase, TNF-α, CD3, FSP-1, α-SMA, cleaved caspase-3) and vessels (CD31) in each slide were calculated by averaging the number of cells per ×400 field in 10 nonoverlapping fields with an upright microscope (BX43, Olympus, Tokyo, Japan). Subsequently, the reactivity of each antibody at time points 0, 24, and 48 h was compared between non-DM and DM. All immunohistochemically stained slides were reviewed by a renal pathologist who was blind to the experimental groups. All data were collected at a magnification of ×400 under the upright microscope.

Statistical analysis. Statistical analysis was performed using two-way analysis of variance, followed by Šidák's multiple comparison test between non-DM and DM at each time point. All analyses were performed using GraphPad Prism 9.0 software (GraphPad, San Diego, CA). $P < 0.05$ was considered statistically significant.

Results

Hematoxylin and eosin staining. All images and description of hematoxylin and eosin staining was reused from our previous study.[28] As shown in Figure 2, the ischemic injury resulted in various patterns of tubular damage, including cytoplasmic vacuolization, brush border loss, and epithelium flattening. In DM monkeys, such injury pattern was observed even prior to IRI. In postischemic samples (24 and 48), coagulation necrosis and extensive hyaline casts were more noticeable in the DM compared with non-DM monkeys.

KI-67. It has been reported that the expression of KI-67 is increased in post-ischemic renal tubular cells in mice.[10,25] However, the change of KI-67-stained tubular cells in monkeys has not been reported previously. DM monkeys had more KI-67-stained cells at baseline, 24 and 48 h than did non-DM monkeys ($P < 0.05$). In contrast, positive cells were rarely found in the non-DM tissues. A significantly higher number of KI-67-positive cells was detected in DM versus non-DM animals at all 3 time points (Figure 3 B) ($P < 0.05$).

Na^+/K^+ ATPase. The expression pattern differed between the DM and non-DM monkeys (Figure 4 A). In baseline samples, its expression was clear in the basolateral area of the tubule in non-DM tissue, while this polarized localization was not present in DM monkeys. Similar findings were observed at 24 h. At 48 h, its expression was no longer detected in the basal membrane in non-DM monkeys, although it was detected at intercellular junctions of tubules. In DM monkeys, its expression in the tubule was uncertain at 48 h, possibly due to the lower number of viable tubules, as also shown by H and E staining (Figure 2). qRT-PCR analysis showed that mRNA expression was similar between the 2 groups at baseline and 24 h, while expression was lower in DM than non-DM at 48 h ($P < 0.05$) (Figure 4 B).

TNF-α. Before ischemic injury, the expression of TNF-α was higher in DM than in non-DM monkeys (Figure 5 A and B, $P < 0.05$). At 24 h, no difference was observed between 2 groups. At 48 h, expression was higher in DM as compared with non-DM monkeys (Figure 5 A and B, $P < 0.05$).

CD31. As shown in Figure 6, the number of clearly visible capillaries was not different between 2 groups before or 24 h after IRI. At 24 and 48 h, collapsed vessels were observed in DM, while most vessels were well-delineated in non-DM monkeys at 24 h (Figure 6 A). At 48 h, significantly fewer CD31-positive vessels were found in DM as compared with non-DM monkeys (Figure 6 A and B, $P < 0.001$).

Table 1. Primer sequences used in this study

Gene	Forward (5′-3′)	Reverse (5′-3′)	Reference or Genbank ID
MRFAP1	GCGGATAGAGAAGAGCGAGT	AGCCAATCTCCACCAGTTGA	38
Na^+/K^+ ATPase	ATTGCCACACTTGCTTCTGG	CCTCAAGCCAGGTGTACTCA	NM_001266673.1
TNF-α	GTCAACCTCCTCTCTGCCAT	CCAAAGTAGACCTGCCCAGA	NM_001047149.1
α-SMA	CTTTCAATGTCCCAGCCATG	CGCTCAGTCAGGATCTTCAT	NM_001258072.1

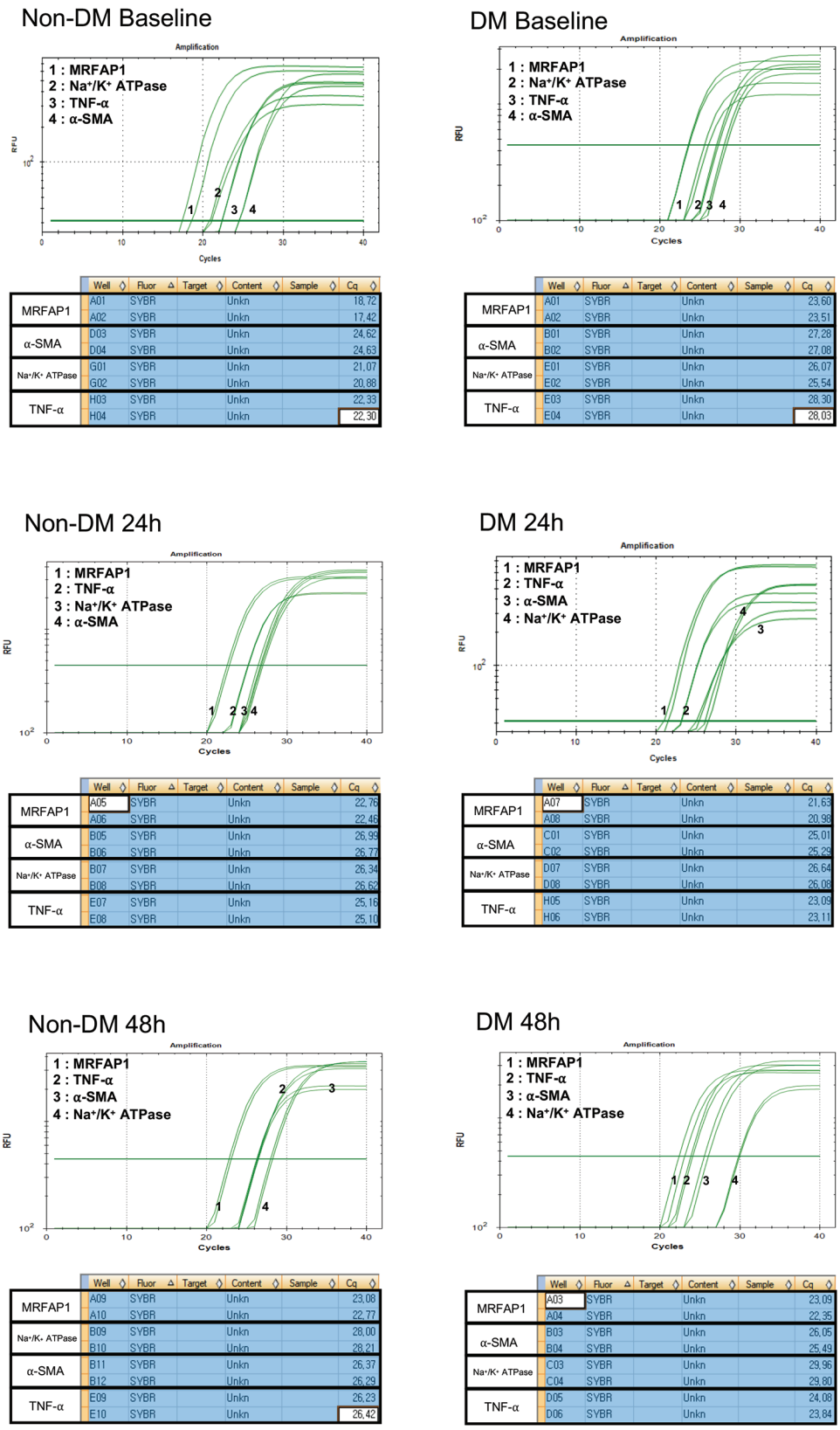

Figure 1. Representative amplification plots of RT-qPCR in logarithmic view. All amplification was conducted in duplicate. The horizontal bar is threshold that was calculated automatically. RFU, relative fluorescence unit.

Table 2. Information on the antibodies and staining kit used in this study

Target	Primary antibody	Secondary antibody and chromogenic kit
KI-67	Ki-67 antibody (D2H10), Cell signaling technology, 9027, 1:500	Mouse and rabbit specific HRP/DAB IHC detection kit - Micropolymer, Abcam, ab236466
Na^+/K^+ ATPase	ATP1A1/ATP1A2/ATP1A3 antibody (H-3), SCBT, sc-48345, 1:500	
TNF-α	TNFα antibody (52B83), SCBT, sc-52746, 1:500	
Cleaved caspase 3	Cleaved caspase-3 (Asp175) antibody, Cell signaling technology, 9661, 1:400	
CD31	Anti-CD31 antibody (RM1006), Abcam, ab281583, 1:4000	
FSP-1	S100A4 recombinant rabbit monoclonal antibody (SD200-08), Invitrogen, 1:100	
CD3	Polyclonal rabbit anti-human CD3, Dako IR503, Ready-to-use	
α-SMA	Antialpha smooth muscle actin antibody, Abcam, ab5694, 1:200	

CD3. As shown in Figure 7, DM monkeys had more CD3-positive cells than non-DM monkeys at 24 and 48 h ($P < 0.0001$), while no difference was detected at baseline. In most cases, the CD3-positive cells were found near the glomeruli.

FSP-1. FSP-1 expression was detected in interstitial area of all samples (Figure 8 A). Its expression was higher in DM as compared with non-DM monkeys at 24 ($P < 0.05$) and 48 h ($P < 0.0001$) (Figure 8 B).

Cleaved caspase 3. Generally, cleaved caspase 3-positive cells were predominantly observed in tubules and glomerulus, with few positive cells in interstitium (Figure 9 A). The numbers of positive cells were not significantly different between 2 groups at baseline, 24 h, and 48 h (Figure 9 B).

α-smooth muscle actin. No difference was found in the pattern of staining in non-DM and DM monkeys at baseline, 24 h, or 48 h (Figure 10 A). Consistent with this, qRT-PCR analysis showed similar expression in non-DM and DM monkeys at baseline, 24 h, and 48 h (Figure 10 B).

Discussion

Recent studies suggest that DM is an independent risk factor for AKI.[18,54] However, relevant studies using large animal models could advance clinical translation.[37] In this study, renal biopsy tissues were obtained from non-DM and DM monkeys before and at 24 and 48 h after IRI. Subsequently, the expression of markers of proliferation (KI-67), apoptosis (cleaved caspase 3), ion exchange (Na^+/K^+ ATPase), inflammation (TNF-α), capillary density (CD31), T-cells (CD3), and fibrotic change (FSP-1 and α-SMA) were compared between DM and non-DM monkeys.

Due to high metabolic demand, renal tubules are susceptible to apoptosis, and loss of tubular function after renal IRI has been reported in small animal models.[45,57] In addition, prolonged hyperglycemia can contribute to increased renal cell death.[14] For example, p53 activation was responsible for the increased apoptosis of tubular cells in diabetic mice after bilateral ischemia.[39] Only a few reports address the occurrence of apoptotic tubules in studies on monkeys. In one study on the cynomolgus monkey, the unilateral IRI (90 min) of the single kidney followed by nephrectomy of the other resulted in the appearance of cleaved caspase-3-positive cells in the overall renal tissue including the cortex, and the outer and inner stripe of the outer medulla, and was most numerous in the outer stripe of the outer medulla at 24 h.[17] From the aforementioned study,[17] the number of apoptotic cells were decreased by being pretreated with melatonin 5 min before IRI, further corroborating that the measurement of the apoptotic death of renal cells is beneficial for determining the progression or recovery of IRI in monkeys. We observed that the number of apoptotic cells were increased to a similar degree at 24 and 48 h in both DM and non-DM monkeys. This observation indicate that underlying DM may not cause increased apoptosis during 48-hour period after IRI, at least in the present protocol

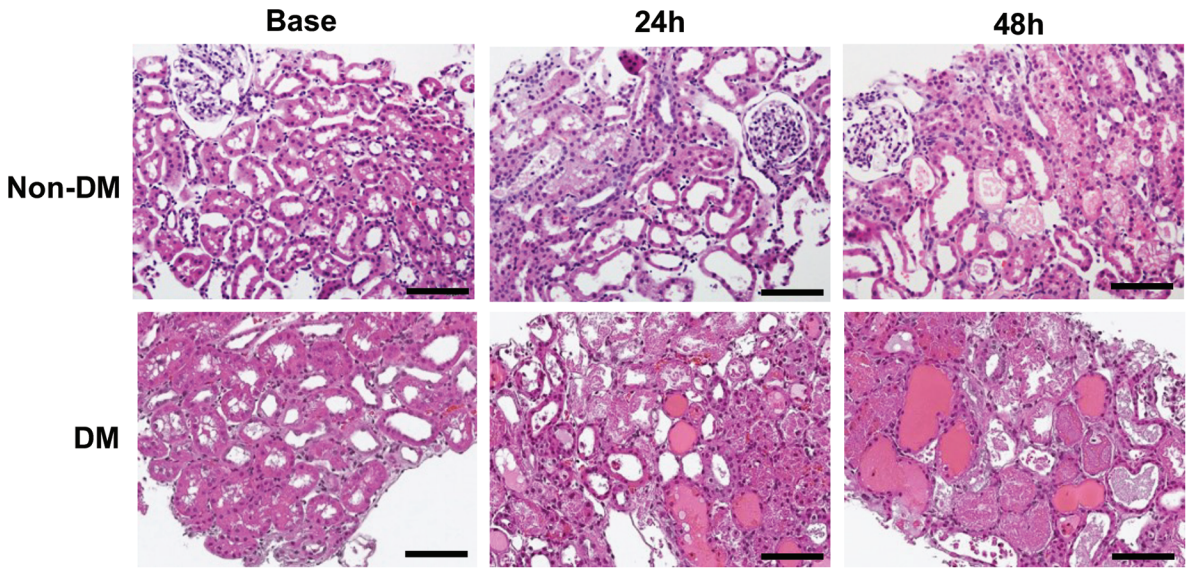

Figure 2. Histologic examination of H&E-stained renal tissues. All images were re-used from our previous study.[28] Scale bar, 100 μm. Original magnification, ×200.

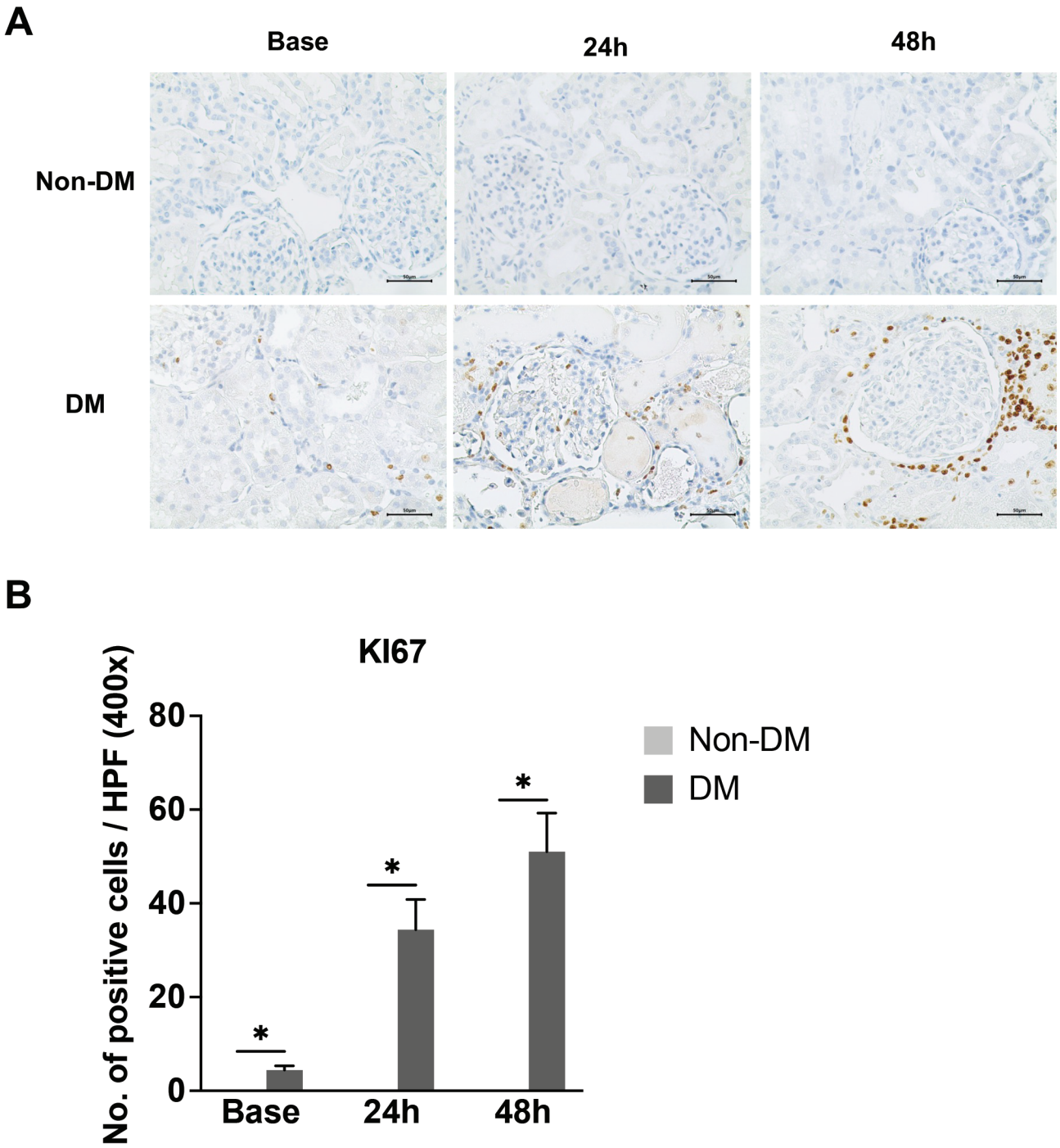

Figure 3. Immunohistochemical detection and quantification of KI-67-positive cells in AKI kidneys. Renal biopsy before and after ischemia/reperfusion injury was obtained from non-DM or DM monkeys(A) Representative images of positive cells in the I/R kidneys at different time points (n = 3). Positively stained cells are colored brown. Hematoxylin was used for nuclear counterstaining. Scale bars, 50 µm. Original magnification, ×400. (B) The changes in the number of KI-67-positive cells within each group were compared (n = 3). *P < 0.05.

(1-h bilateral clamping) in monkeys. Further studies would be needed to delineate the relationship between diabetes and the increased susceptibility of AKI.[54]

Tubular cells are generated from surviving nearby cells after injury.[3] Many studies have shown through staining with PCNA, Cyclin D1, or KI-67 that cells enter the G1 phase after injury, indicating that tubular cells can potentially reenter the cell cycle.[51] KI-67 or PCNA expressions have been commonly used to assess the proliferation of tubules. For example, PCNA was more abundantly observed in glomerulonephritis, and its potential use for the assessment of mesangial proliferation was suggested.[34] Similarly, the expression of PCNA in renal biopsy tissue from lupus nephritis patients was associated with disease activity and chronicity, and suggested value of this marker for prognosis.[25] Experimentally, the patterns of PCNA expression are mostly dependent on the study protocol used. A 30-min bilateral IRI in mice showed 2 waves of renal cell proliferation; most KI-67-positive cells were interstitial fibroblasts and tubular

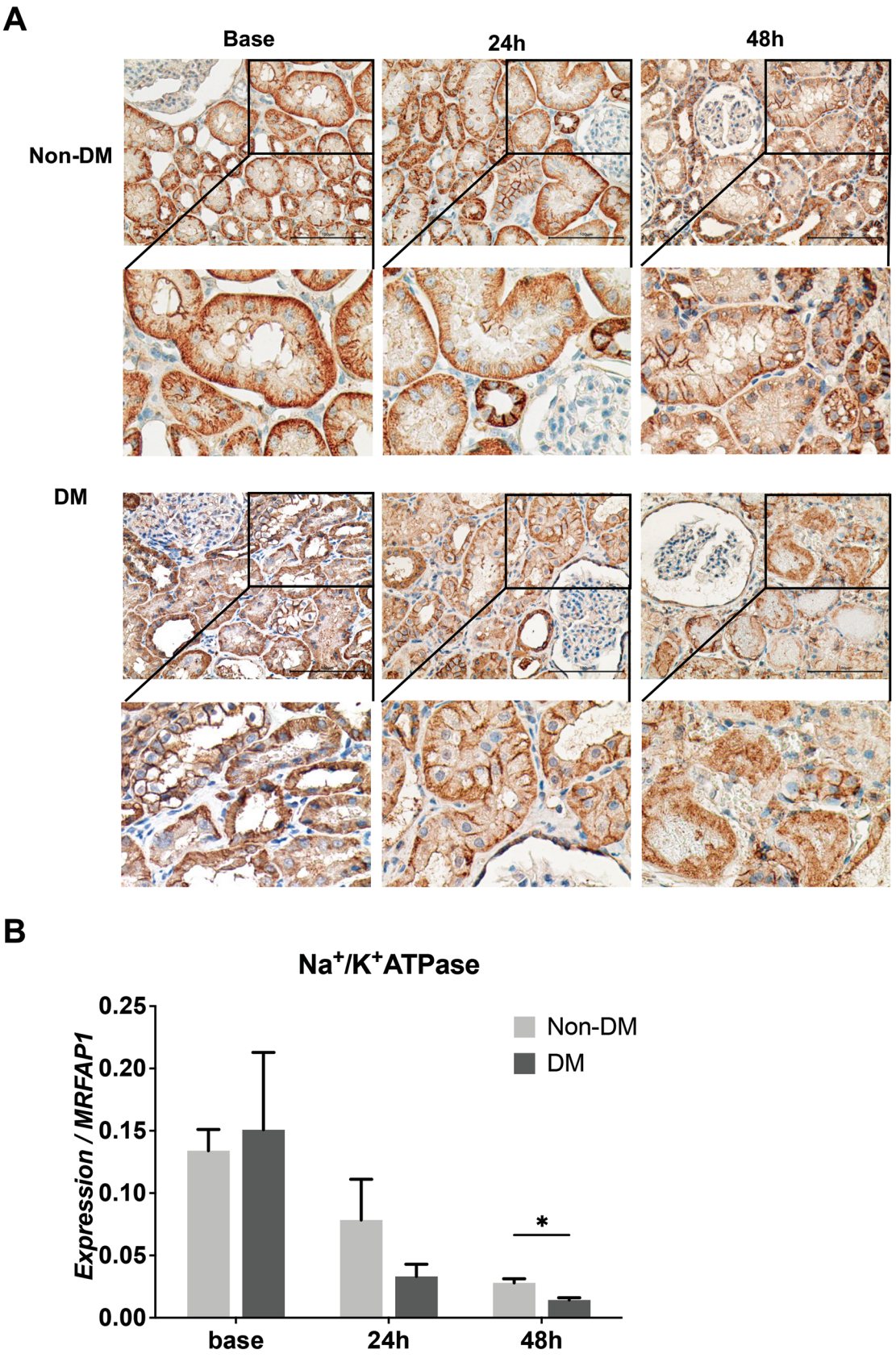

Figure 4. Immunohistochemical detection and qRT-PCR analysis of Na^+/K^+ ATPase expression in AKI kidneys. Renal biopsy before and after ischemia/reperfusion injury was obtained from non-DM or DM monkeys. (A) Representative images of Na^+/K^+ ATPase protein expression in the I/R kidneys at different time points ($n = 3$). Positively stained cells are colored brown. Hematoxylin was used for nuclear counterstaining. Scale bars, 100 μm. Original magnification, ×400. (B) qRT-PCR analysis of Na^+/K^+ ATPase. The expression of Na^+/K^+ ATPase was normalized to that of MRFAP1 ($n = 3$). *$P < 0.05$.

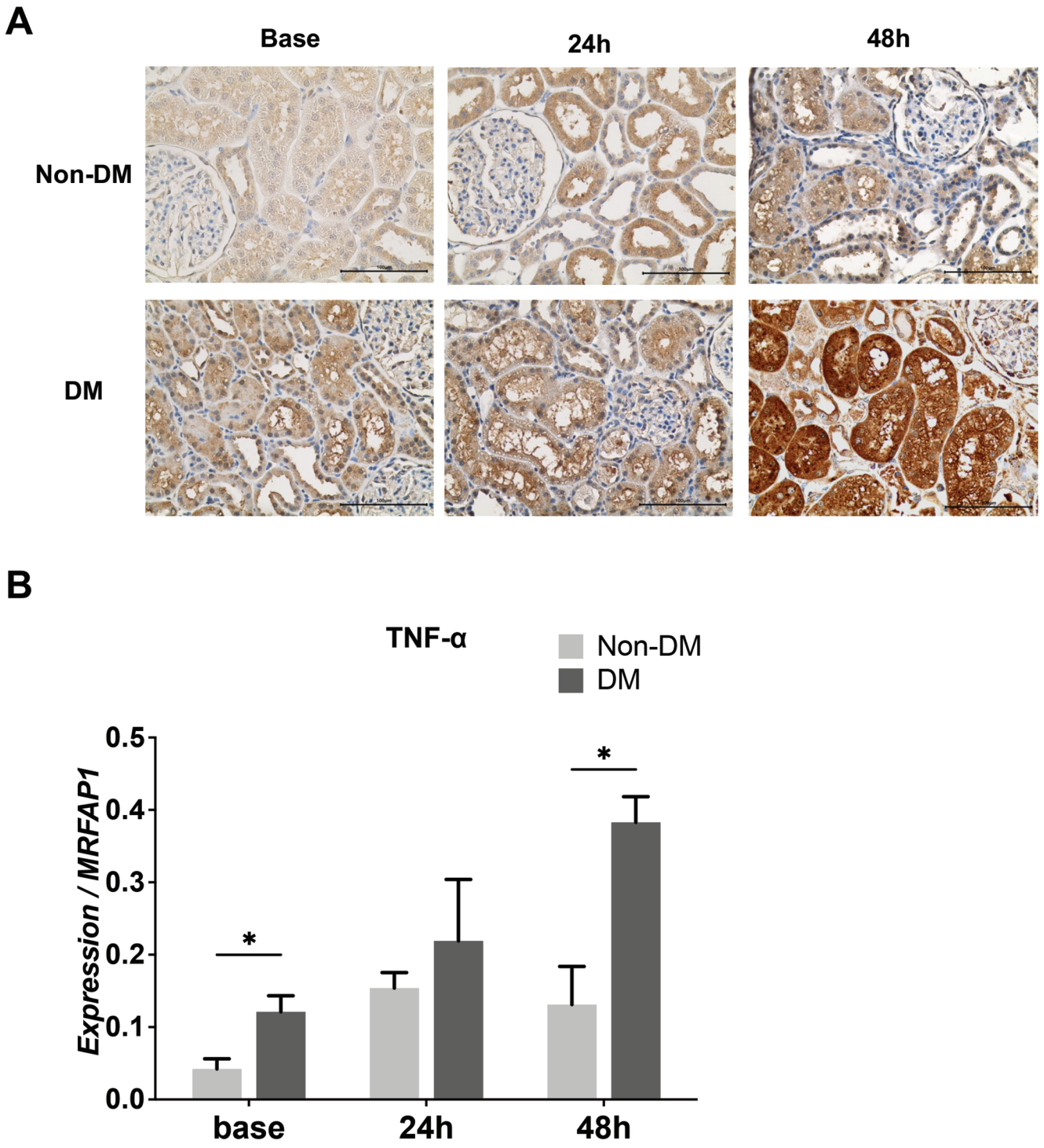

Figure 5. Immunohistochemical detection and qRT-PCR analysis of TNF-α in AKI kidneys. Renal biopsy before and after ischemia/reperfusion injury was obtained from non-DM or DM monkeys. (A) Representative images of TNF-α expression in the I/R kidneys at different time points ($n = 3$). Positively stained cells are colored brown. Hematoxylin was used for nuclear counterstaining. Scale bars, 100 µm. Original magnification, ×400. (B) qRT-PCR analysis of TNF-α in renal tissues. The expression of TNF-α was normalized to that of MRFAP1 ($n = 3$). *$P < 0.05$.

cells at 12 h and 3 d, respectively, after IRI.[55,56] Another study showed that in mice with a unilateral 45-min ischemia, only day 7 showed a marked increase in KI-67-expressing cells as compared with the contralateral control kidney, with no difference at 3 h and 1 d after IRI.[45] In line with these reports, we found that IRI increased the number of cells undergoing proliferation in DM monkeys but not in non-DM monkeys. This finding indicates that the sensitivity to ischemic insult differs between non-DM and DM. Although informative, the use of cell cycle markers such as KI-67, PCNA, or histone H3 phosphorylation may not reveal whether the cell division has actually occurred because these markers cannot distinguish between cells that initiate division and those that actually produce 2 daughter cells. Even cells that are arrested after the S phase are likely to

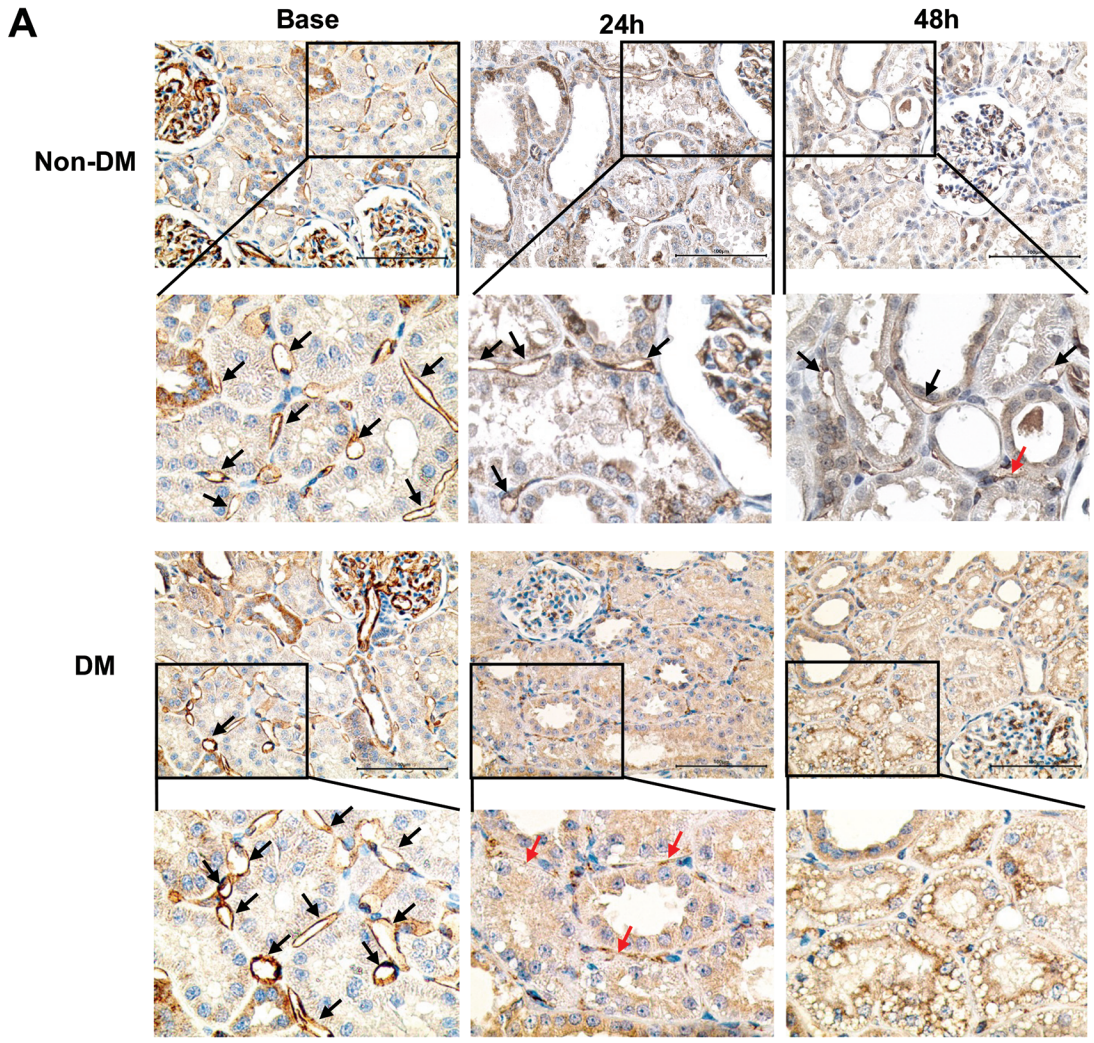

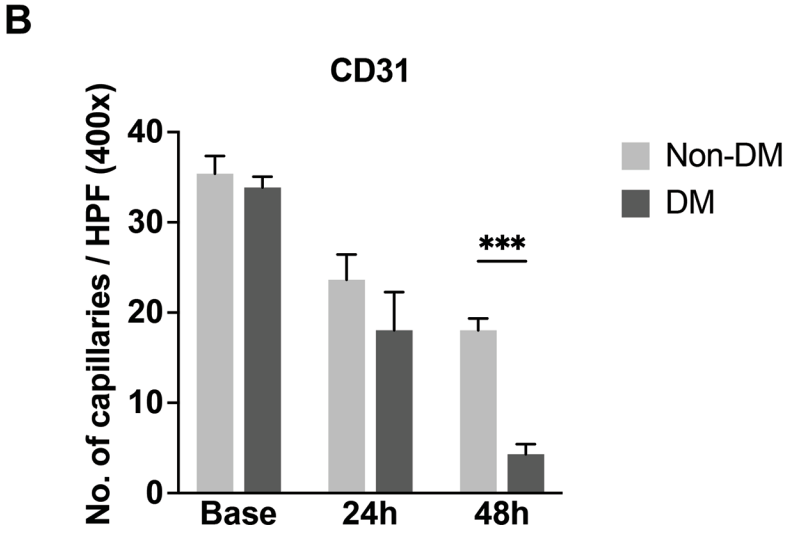

Figure 6. Immunohistochemical detection and quantification of capillary density in AKI kidneys. Renal biopsy before and after ischemia/reperfusion injury was obtained from non-DM or DM monkeys. CD31 antibody was used. (A) Representative images of CD31-expressing microvessels in the I/R kidneys at different time points. Positively stained cells are colored brown. Hematoxylin was used for nuclear counterstaining. Black arrows, vessels with normal integrity; red arrows, collapsed vessels. (B) The number of microvessels with normal integrity was compared ($n = 3$). Scale bars, 100 μm. Original magnification, ×400. ***$P < 0.001$.

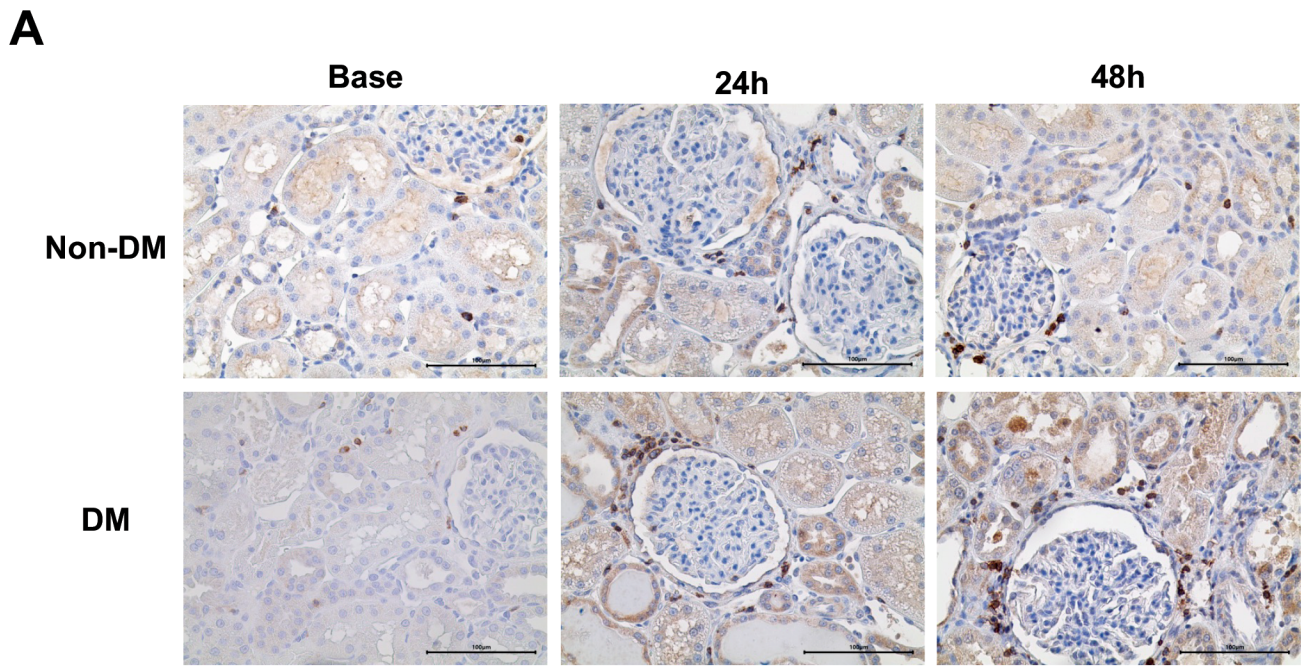

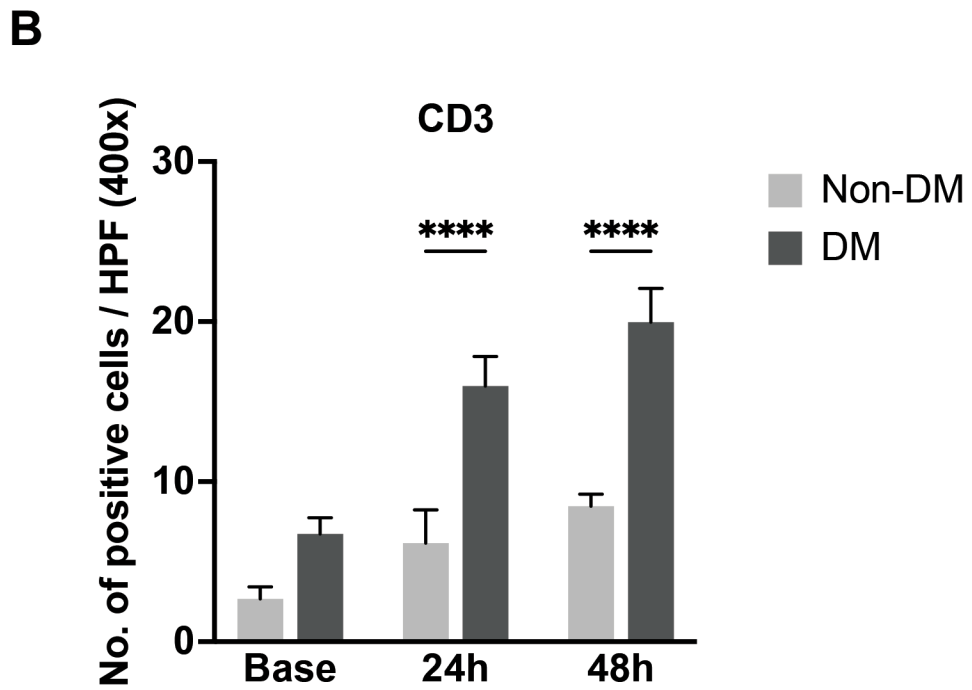

Figure 7. Immunohistochemical detection and quantification of CD3 in AKI kidneys. Renal biopsy before and after ischemia/reperfusion injury was obtained from non-DM or DM monkeys. CD3 antibody was used. Positively stained cells are colored brown. Hematoxylin was used for nuclear counterstaining. (A) Representative images of CD3-expressing cells in the I/R kidneys at different time points. (B) The number of CD3-expressing cells in the renal tissue was compared (n = 3). Scale bars, 100 µm. Original magnification, ×400. ****$P < 0.0001$.

be stained with these markers.[8] Investigation using technical methods such as a fluorescent reporter combined with cell cycle analysis is necessary to distinguish progressive and arrested proliferation, thus clearly validating the value of this marker.[8]

Various physiologic insults cause damages of membrane-bound proteins. In the kidney, it was reported that the expression of Na^+/K^+ ATPase was reduced by radiation- and ischemia-induced renal injury.[21,50] One of the most notable changes of this ion transport channel after ischemic injury is the reduction of its expression and its translocation from basolateral area to apical side of the cell.[50] For example, in a rat model of renal ischemia and reperfusion, the immune-detectable level

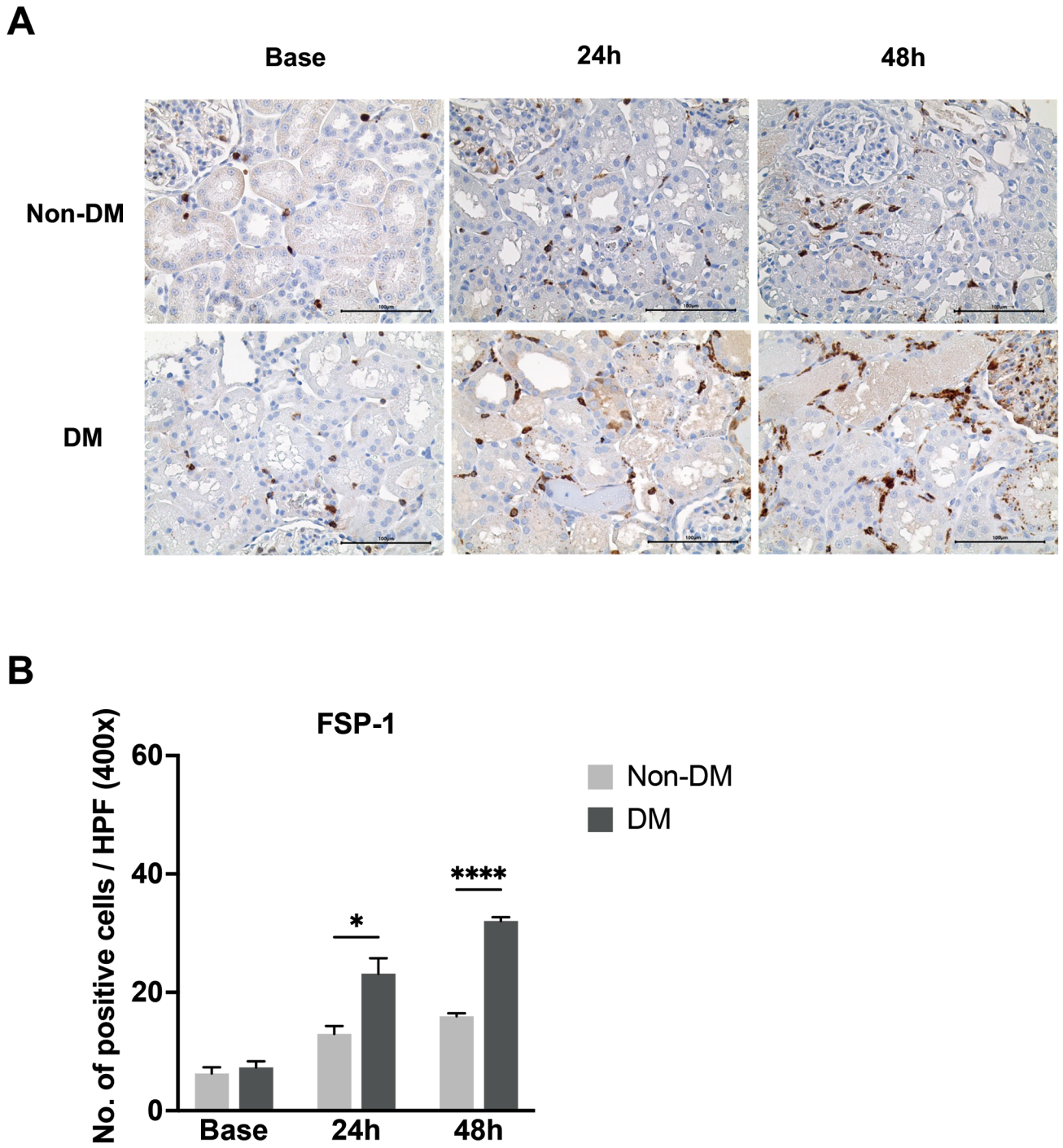

Figure 8. Immunohistochemical detection and quantification of FSP1-expressing cells in AKI kidneys. Renal biopsy before and after ischemia/reperfusion injury was obtained from non-DM or DM monkeys. (A) Representative images of FSP1-expressing cells in the I/R kidneys at different time points. Positively stained cells are colored brown. Hematoxylin was used for nuclear counterstaining. (B) The number of FSP1-expressing cells in the renal tissue was compared ($n = 3$). Scale bars, 100 µm. Original magnification ×400. *$P < 0.05$ and ****$P < 0.0001$.

of Na^+/K^+ ATPase at 6 h, fell sharply after the injury, followed by recovery to 60% to 70% level of the nonischemic control at 24 h.[50] The effect of DM on Na^+/K^+ ATPase expression has not been reported to date. We found that its expression in basal area of tubule was not clearly discerned in DM monkeys even before ischemia and became weak and diffuse during 48 h period of reperfusion. These findings suggest that DM affects the post-ischemic localization of this pump or disrupting the polarity of renal epithelial cells.[53]

Renal epithelial cells can produce inflammatory cytokines (for example, TNF-α, IL-6, MCP-1, CXCL1) in response to ischemic injury. A central role for TNF-α in AKI was demonstrated by resistance to AKI in TNF-α-knockout mice.[40] We previously showed that the level of serum TNF-α remained constant for 48 h in non-DM monkeys, with large variance within the group.[28] The current results indicate that its expression was higher in DM than non-DM monkeys, even before IRI. The mechanism for increased TNF-α in baseline samples in DM is not clear.

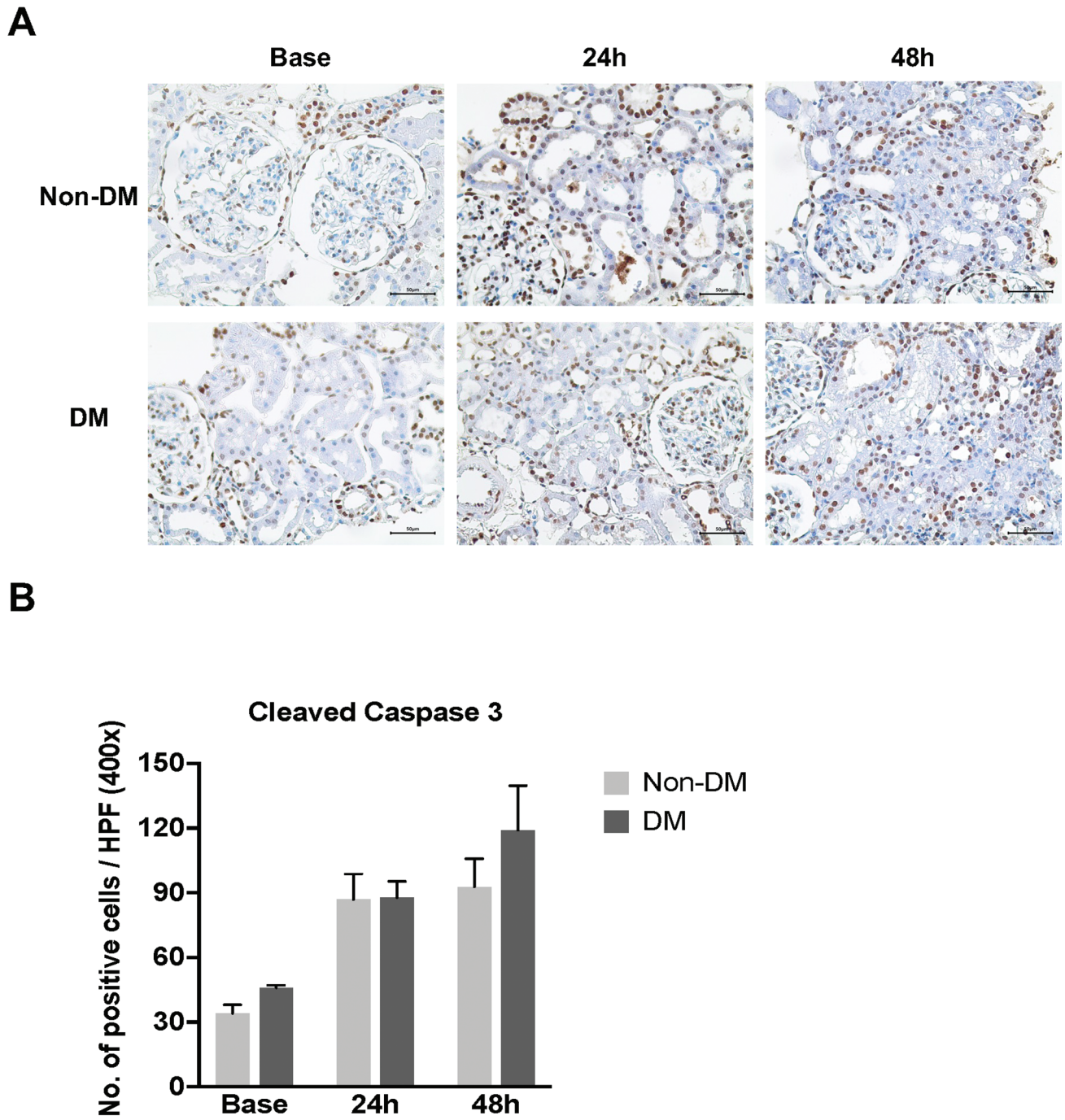

Figure 9. Immunohistochemical detection and quantification of caspase 3-positive cells in AKI kidneys. Renal biopsy before and after ischemia/reperfusion injury was obtained from non-DM or DM monkeys and the positive cells were detected using antibody against cleaved caspase 3. (A) Representative images of cleaved caspase-3-positive cells in the I/R kidneys at different time points. Positively stained cells are colored brown. Hematoxylin was used for nuclear counterstaining. (B) The change in number of positive cells was compared within each group. Scale bars, 50 µm. Original magnification, ×400.

Advanced glycan end products or oxidation products could possibly have caused an innate immune response in the DM kidney, which caused inflammation in renal cells.[12,43] At 48 h after IRI, TNF-α expression was markedly higher in DM monkeys, consistent with previous findings in rodent studies.[5,12] These results indicate that the severity of AKI in DM monkeys may have been due to a constantly higher level of TNF-α; this possibility is supported by renal injury scores, urinary albumin, and *Ngal* mRNA expression in renal tissue.[28]

T-cells contribute to the establishment of AKI during the early phase of IRI.[29] CD4-deficient mice showed attenuated renal tubular injury after IRI.[4] Moreover, postischemic injury and macrophage infiltration was restored by adoptive transfer of $CD4^+$ T cells, indicating that T-cells are a key mediator of ischemic injury.[4] Another study showed that mice with unilateral ischemia and immediate contralateral kidney nephrectomy had more CD3-positive cells 3 days after injury.[9] Another study showed that $CD3^+$ T cells were more abundant in type 2 diabetic

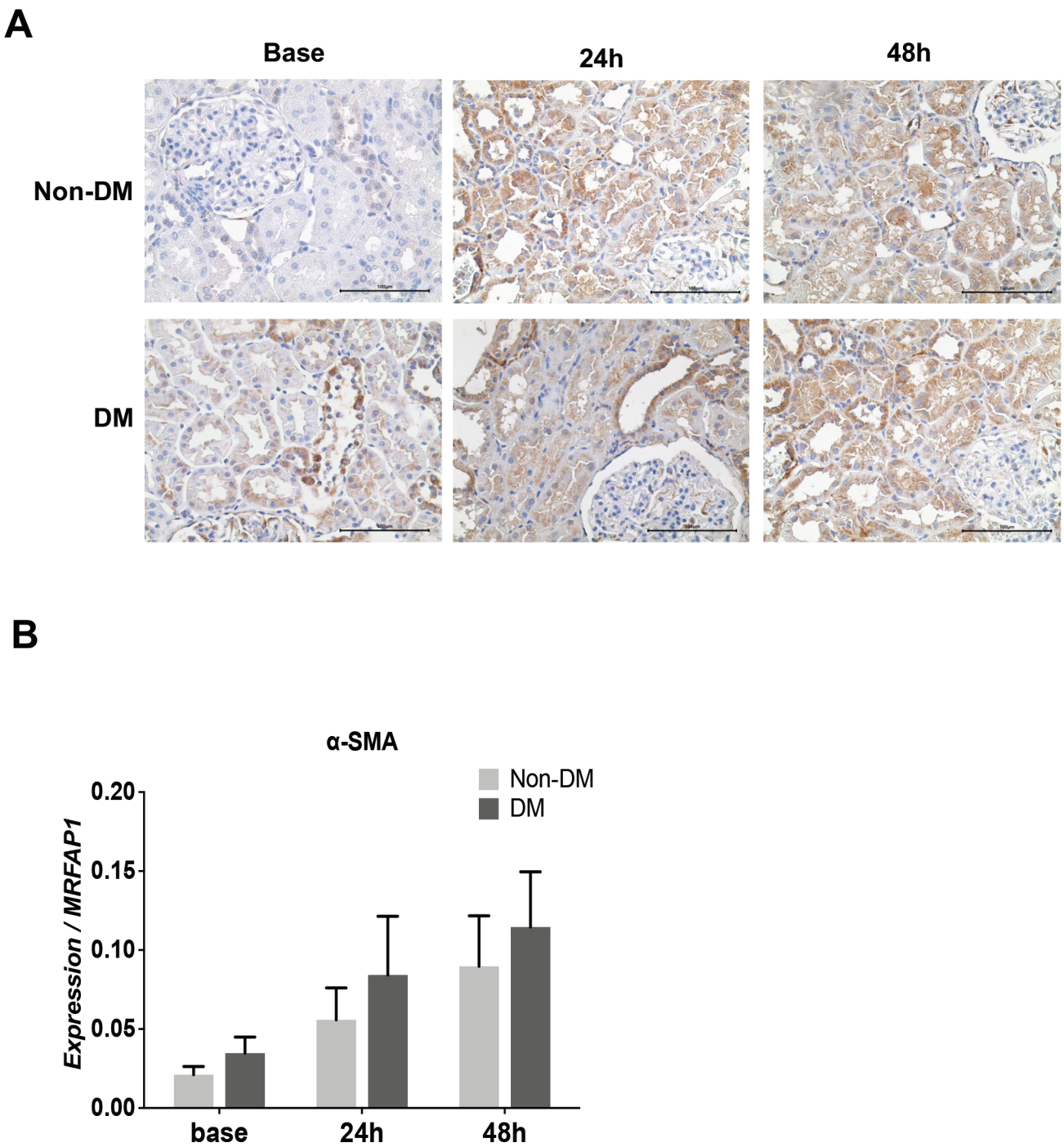

Figure 10. Immunohistochemical detection and qRT-PCR analysis of α-SMA in AKI kidneys. Renal biopsy before and after ischemia/reperfusion injury was obtained from non-DM or DM monkeys. (A) Representative images of α-SMA expression in the I/R kidneys at different time points ($n = 3$). Positively stained cells are colored brown. Hematoxylin was used for nuclear counterstaining. Scale bars, 100 μm. Original magnification, ×400. (B) qRT-PCR analysis of α-SMA in renal tissues. The expression of α-SMA was normalized to that of MRFAP1 ($n = 3$).

rats than in non-DM controls.[33] These results are consistent with the present results showing more infiltrated T cells in the renal tissue of DM monkeys. Further studies could detail on the distribution of CD3 subsets ($CD3^+/CD4^+$, $CD3^+/CD8^+$, and $CD3^+/CD4^-/CD8^-$ T cells).[19]

Epithelial cells undergo mesenchymal changes after prolonged exposure to high glucose.[36] The number of FSP-1-expressing cells in the interstitium was increased in DM monkeys. However, the expression of α-SMA,[16] another marker for mesenchymal change, was not affected by ischemic injury. From this observation, it can be suggested that FSP-1-positive cells appear acutely after IRI in DM kidney, although mesenchymal change did not occur in the tubules. It was reported that FSP-1-expressing cells can also be derived from bone marrow or resident fibroblasts, which contribute to renal fibrosis.[27] Further study is needed to determine how hyperglycemia affects the function of FSP-1 early in renal ischemic injury.

AKI capillary reduction was significant in DM monkeys at 24 and 48 h after AKI. The number of morphologically intact vessels was sharply lower in DM than non-DM at 24 h of IRI,

which may have impeded the recovery of AKI.[28] The decrease in vascular density after AKI has promotes hypoxia, impairs hemodynamic responses, and predisposes patients to chronic kidney disease (CKD) and hypertension.[30] Moreover, animal studies have demonstrated that underlying CKD aggravates the loss of capillary after AKI.[23] Considering that high blood glucose and its by-products (for example, advanced glycation end products) are independent risk factors for endothelial cell damage in renal vessels, assessment of the glycation level and the structural integrity of endothelial cells in glomerulus, peritubular capillaries, and large renal vessels would be required.[11]

The progression of AKI induced by renal IRI depends on various procedural factors (e.g., post-procedural time, whether one or both kidneys were clamped, and whether or not the nonclamped kidney was removed), and monkey protocols can differ depending on the purpose of the experiment. One group examined the effect of pretreating with erythropoietin before renal IRI in cynomolgus monkeys, performing a right nephrectomy followed by a left unilateral IRI for 90 min.[17] Under this protocol, the serum creatinine was highest at 24 h (> 6.0 mg/dL) and then gradually decreases. That protocol differs from ours, in which the peak creatinine level occurred at 48 h in both DM and non-DM monkeys.[28] The smaller increase in creatinine in our study is likely due to less ischemia time (1 h compared with 1.5 h), and the number of kidneys affected (bilateral simultaneous clamping compared with nephrectomy followed by unilateral clamping of contralateral side). Another group induced a warm ischemic injury (35 to 45 min) followed by a 2 h cold ischemic injury in isolated kidney, with the ureter intact, followed by orthotropic auto-transplantation and nephrectomy of the contralateral side.[7] This protocol is more clinically relevant to transplantation cases that use marginal donors that underwent warm and cold ischemia, although the model does not engender allogenic responses. In the study,[7] some animals showed 2- to 4-fold increases in serum creatinine levels, although with large variance.

Additional studies of infiltrating immune cells, other membrane channel proteins, inflammatory membrane proteins (E-selectin, ICAM-1, VCAM-1),[6] and endothelial cells in the glomerulus and peritubular capillaries would help to elucidate the effect of the underlying hyperglycemia on AKI progression. However, commercially available antibodies cannot always be used in monkeys due to lack of cross-reactivity between species, thereby complicating result interpretation from results. Furthermore, the limited volume of biopsy tissue in turn limits the number of available tissue sections. In addition, performing a biopsy can cause bleeding or local inflammation,[15] which may cause additional changes in the tissue. In this regard, the identification of noninvasive molecular markers with relatively high specificity and sensitivity would be an ideal alternative to tissue biopsy.[35]

Immunohistochemical analysis allows the visualization of target protein expression in the context of tissue microstructure. Thus, immunohistochemistry (IHC) has been an important tool for basic and clinical research (for example, evaluation of diagnostic biomarkers).[24] However, IHC is subject to many variables (for example, specimen collection, fixation, preparing paraffin blocks, antigen retrieval, blocking, antibody selection, and chromogenic procedure, etc.) that can complicate analysis and yield divergent results.[49] Thus, results should be interpreted cautiously. Relevant to the present study, ischemia of biopsied specimen before fixation reportedly can cause the breakdown of protein by activation of protease.[44] Furthermore, the reactivity of KI-67 can reportedly be altered by the tissue handling of surgical specimen (e.g., pre-fixation time and duration of fixation) after tissue collection.[2] Therefore, the sharp increase of KI-67-positive cells after AKI in DM samples may have been partly due to the combined effect of DM and tissue handling procedures. The results from other quantitative evaluation methods (immunoblotting or qRT-PCR, etc.) would be needed to identify the possible variations in the IHC results.

In conclusion, we showed that DM promotes the progression of renal ischemia/reperfusion injury by stimulating tubular cell proliferation, reducing capillary density, increasing T cell infiltration, as well as altering protein and mRNA expression of various genes involved ion channel, inflammation, and fibrotic change. The results from this nonhuman primate study are relevant to understanding how DM potentiates the development and progression of AKI.

Acknowledgments

This work was supported by a National Research Foundation of Korea (NRF) grant funded by the Korean government (MSIT) (2021R1A2C2093867). This research was supported by a grant from the Korean Health Technology R&D Project through the Korean Health Industry Development Institute (KHIDI), funded by the Ministry of Health & Welfare, Republic of Korea (Grant Number: HI20C0056). The authors also thank Designed Animal Research Center, Institutes of Green-Bio Science and Technology, Seoul National University, for the technical supports during tissue preparation.

The top 6 panels in Figure 2 of this manuscript were originally published as part of Figure 2 in reference 28 of this manuscript. Some text from the Materials and Methods section was also reused from reference 28. This material is used in this manuscript courtesy of Hindawi Publishing under the Creative Commons Attribution License, version 4 (https://creativecommons.org/licenses/by/4.0/). Use of Figure 2 in this manuscript is available without charge subject to the same Creative Commons license.

References

1. **Animal Welfare Act as Amended.** 2008. 7 USC §2131–2156.
2. **Arima N, Nishimura R, Osako T, Nishiyama Y, Fujisue M, Okumura Y, Nakano M, Tashima R, Toyozumi Y.** 2016. The importance of tissue handling of surgically removed breast cancer for an accurate assessment of the Ki-67 index. J Clin Pathol **69**:255–259. https://doi.org/10.1136/jclinpath-2015-203174.
3. **Berger K, Bangen JM, Hammerich L, Liedtke C, Floege J, Smeets B, Moeller MJ.** 2014. Origin of regenerating tubular cells after acute kidney injury. Proc Natl Acad Sci USA **111**:1533–1538. https://doi.org/10.1073/pnas.1316177111.
4. **Burne MJ, Daniels F, El Ghandour A, Mauiyyedi S, Colvin RB, O'Donnell MP, Rabb H.** 2001. Identification of the CD4+ T cell as a major pathogenic factor in ischemic acute renal failure. J Clin Invest **108**:1283–1290. https://doi.org/10.1172/JCI200112080.
5. **Cheng D, Liang R, Huang B, Hou J, Yin J, Zhao T, Zhou L, Wu R, Qian Y, Wang F.** 2021. Tumor necrosis factor-alpha blockade ameliorates diabetic nephropathy in rats. Clin Kidney J **14**:301–308. https://doi.org/10.1093/ckj/sfz137.
6. **Cheng H, Harris R.** 2014. Renal endothelial dysfunction in diabetic nephropathy. Cardiovasc Hematol Disord Drug Targets **14**:22–33. https://doi.org/10.2174/1871529X14666140401110841.
7. **Da Silva M, Petruzzo P, Virieux S, Tiollier J, Badet L, Martin X.** 2001. A primate model of renal ischemia-reperfusion injury for preclinical evaluation of the antileukocyte function associated antigen 1 monoclonal antibody odulimonab. J Urol **166**:1915–1919. https://doi.org/10.1016/S0022-5347(05)65720-5.
8. **De Chiara L, Conte C, Antonelli G, Lazzeri E.** 2021. Tubular cell cycle response upon AKI: Revising old and new paradigms to identify novel targets for CKD prevention. Int J Mol Sci **22**:11093. https://doi.org/10.3390/ijms222011093.
9. **do Valle Duraes F, Lafont A, Beibel M, Martin K, Darribat K, Cuttat R, Waldt A, Naumann U, Wieczorek G, Gaulis S, Pfister S, Mertz KD, Li J, Roma G, Warncke M.** 2020. Immune cell

landscaping reveals a protective role for regulatory T cells during kidney injury and fibrosis. JCI Insight **5**:e130651. https://doi.org/10.1172/jci.insight.130651.

10. **Dong Y, Zhang Q, Wen J, Chen T, He L, Wang Y, Yin J, Wu R, Xue R, Li S, Fan Y, Wang N.** 2019. Ischemic duration and frequency determines AKI-to-CKD progression monitored by dynamic changes of tubular biomarkers in IRI mice. Front Physiol **10**:153. https://doi.org/10.3389/fphys.2019.00153.
11. **Dou L, Jourde-Chiche N.** 2019. Endothelial toxicity of high glucose and its by-products in diabetic kidney disease. Toxins (Basel) **11**:578. https://doi.org/10.3390/toxins11100578.
12. **Gao G, Zhang B, Ramesh G, Betterly D, Tadagavadi RK, Wang W, Reeves WB.** 2013. TNF-alpha mediates increased susceptibility to ischemic AKI in diabetes. Am J Physiol Renal Physiol **304**:F515–F521. https://doi.org/10.1152/ajprenal.00533.2012.
13. **Gaschen L, Menninger K, Schuurman HJ.** 2000. Ultrasonography of the normal kidney in the cynomolgus monkey (*Macaca fascicularis*): Morphologic and Doppler findings. J Med Primatol **29**:76–84. https://doi.org/10.1034/j.1600-0684.2000.290205.x.
14. **Habib SL.** 2013. Diabetes and renal tubular cell apoptosis. World J Diabetes **4**:27–30. https://doi.org/10.4239/wjd.v4.i2.27.
15. **Hull KL, Adenwalla SF, Topham P, Graham-Brown MP.** 2022. Indications and considerations for kidney biopsy: An overview of clinical considerations for the non-specialist. Clin Med (Lond) **22**:34–40. https://doi.org/10.7861/clinmed.2021-0472.
16. **Ina K, Kitamura H, Tatsukawa S, Fujikura Y.** 2011. Significance of alpha-SMA in myofibroblasts emerging in renal tubulointerstitial fibrosis. Histol Histopathol **26**:855–866.
17. **Ishii Y, Sawada T, Murakami T, Sakuraoka Y, Shiraki T, Shimizu A, Kubota K, Fuchinoue S, Teraoka S.** 2011. Renoprotective effect of erythropoietin against ischaemia-reperfusion injury in a non-human primate model. Nephrol Dial Transplant **26**:1157–1162. https://doi.org/10.1093/ndt/gfq601.
18. **James MT, Grams ME, Woodward M, Elley CR, Green JA, Wheeler DC, de Jong P, Gansevoort RT, Levey AS, Warnock DG, Sarnak MJ.** 2015. A Meta-analysis of the association of estimated GFR, albuminuria, diabetes mellitus, and hypertension with acute kidney injury. Am J Kidney Dis **66**:602–612. https://doi.org/10.1053/j.ajkd.2015.02.338.
19. **Jang HR, Rabb H.** 2015. Immune cells in experimental acute kidney injury. Nat Rev Nephrol **11**:88–101. https://doi.org/10.1038/nrneph.2014.180.
20. **Johnson F, Phillips D, Talabani B, Wonnacott A, Meran S, Phillips AO.** 2016. The impact of acute kidney injury in diabetes mellitus. Nephrology (Carlton) **21**:506–511. https://doi.org/10.1111/nep.12649.
21. **Kaločayová B, Kovačičová I, Radošinská J, Tóthóvá L, Jagmaševič-Mézešová L, Fülöp M, Slezák J, Babál P, Janega P, Vrbjar N.** 2019. Alteration of renal Na,K-ATPase in rats following the mediastinal gamma-irradiation. Physiol Rep **7**:e13969. https://doi.org/10.14814/phy2.13969.
22. **Kelly KJ, Burford JL, Dominguez JH.** 2009. Postischemic inflammatory syndrome: A critical mechanism of progression in diabetic nephropathy. Am J Physiol Renal Physiol **297**:F923–F931. https://doi.org/10.1152/ajprenal.00205.2009.
23. **Kida Y.** 2020. Peritubular capillary rarefaction: An underappreciated regulator of CKD progression. Int J Mol Sci **21**:8255. https://doi.org/10.3390/ijms21218255.
24. **Kim SW, Roh J, Park CS.** 2016. Immunohistochemistry for pathologists: Protocols, pitfalls, and tips. J Pathol Transl Med **50**:411–418. https://doi.org/10.4132/jptm.2016.08.08.
25. **Kirim S, Paydas S, Gönlüsen G, Tetiker T.** 2005. Apoptosis and proliferating cell nuclear antigen in lupus nephritis (Class IV) and membranoproliferative glomerulonephritis. Ren Fail **27**:107–113. https://doi.org/10.1081/JDI-42724.
26. **Kumar S.** 2018. Cellular and molecular pathways of renal repair after acute kidney injury. Kidney Int **93**:27–40. https://doi.org/10.1016/j.kint.2017.07.030.
27. **LeBleu VS, Taduri G, O'Connell J, Teng Y, Cooke VG, Woda C, Sugimoto H, Kalluri R.** 2013. Origin and function of myofibroblasts in kidney fibrosis. Nat Med **19**:1047–1053. https://doi.org/10.1038/nm.3218.
28. **Lee KW, Kim TM, Kim KS, Lee S, Cho J, Park JB, Kwon GY, Kim SJ.** 2018. Renal ischemia-reperfusion injury in a diabetic monkey model and therapeutic testing of human bone marrow-derived mesenchymal stem cells. J Diabetes Res **2018**:5182606. https://doi.org/10.1155/2018/5182606.
29. **Lee SA, Noel S, Sadasivam M, Hamad ARA, Rabb H.** 2017. Role of immune cells in acute kidney injury and repair. Nephron **137**:282–286. https://doi.org/10.1159/000477181.
30. **Li S, Wang F, Sun D.** 2021. The renal microcirculation in chronic kidney disease: Novel diagnostic methods and therapeutic perspectives. Cell Biosci **11**:90. https://doi.org/10.1186/s13578-021-00606-4.
31. **Lindström NO, McMahon JA, Guo J, Tran T, Guo Q, Rutledge E, Parvez RK, Saribekyan G, Schuler RE, Liao C, Kim AD, Abdelhalim A, Ruffins SW, Thornton ME, Baskin L, Grubbs B, Kesselman C, McMahon AP.** 2018. Conserved and divergent features of human and mouse kidney organogenesis. J Am Soc Nephrol **29**:785–805. https://doi.org/10.1681/ASN.2017080887.
32. **Livak KJ, Schmittgen TD.** 2001. Analysis of relative gene expression data using real-time quantitative PCR and the 2(-Delta Delta C(T)). Methods **25**:402–408. https://doi.org/10.1006/meth.2001.1262.
33. **Muroya Y, He X, Fan L, Wang S, Xu R, Fan F, Roman RJ.** 2018. Enhanced renal ischemia-reperfusion injury in aging and diabetes. Am J Physiol Renal Physiol **315**:F1843–F1854. https://doi.org/10.1152/ajprenal.00184.2018.
34. **Nakopoulou L, Stefanaki K, Salpigidis K, Boletis J, Papadakis J, Zeiss PM, Vosnides G.** 1997. The value of proliferating cell nuclear antigen (PCNA)-cyclin in the assessment of cell proliferation in glomerulonephritis. Histol Histopathol **12**:655–662.
35. **Nielsen PM, Eldirdiri A, Bertelsen LB, Jorgensen HS, Ardenkjaer-Larsen JH, Laustsen C.** 2017. Fumarase activity: An in vivo and in vitro biomarker for acute kidney injury. Sci Rep **7**:40812. https://doi.org/10.1038/srep40812.
36. **Okada H, Danoff TM, Kalluri R, Neilson EG.** 1997. Early role of Fsp1 in epithelial-mesenchymal transformation. Am J Physiol **273**:F563–F574. https://doi.org/10.1152/ajprenal.1997.273.4.F563.
37. **Packialakshmi B, Stewart IJ, Burmeister DM, Chung KK, Zhou X.** 2020. Large animal models for translational research in acute kidney injury. Ren Fail **42**:1042–1058. https://doi.org/10.1080/0886022X.2020.1830108.
38. **Park SJ, Kim YH, Huh JW, Lee SR, Kim SH, Kim SU, Kim JS, Jeong KJ, Kim KM, Kim HS, Chang KT.** 2013. Selection of new appropriate reference genes for RT-qPCR analysis via transcriptome sequencing of cynomolgus monkeys (*Macaca fascicularis*). PLoS One **8**:e60758. https://doi.org/10.1371/journal.pone.0060758.
39. **Peng J, Li X, Zhang D, Chen JK, Su Y, Smith SB, Dong Z.** 2015. Hyperglycemia, p53, and mitochondrial pathway of apoptosis are involved in the susceptibility of diabetic models to ischemic acute kidney injury. Kidney Int **87**:137–150. https://doi.org/10.1038/ki.2014.226.
40. **Ramesh G, Reeves WB.** 2002. TNF-alpha mediates chemokine and cytokine expression and renal injury in cisplatin nephrotoxicity. J Clin Invest **110**:835–842. https://doi.org/10.1172/JCI200215606.
41. **Rao VRALBV, Tan SH, Candasamy M, Bhattamisra SK.** 2019. Diabetic nephropathy: An update on pathogenesis and drug development. Diabetes Metab Syndr **13**:754–762. https://doi.org/10.1016/j.dsx.2018.11.054.
42. **Institute for Laboratory Animal Research.** 2011. Guide for the Care and Use of Laboratory Animals, 8th ed. Washington (DC): National Academic Press.
43. **Rosin DL, Okusa MD.** 2011. Dangers within: DAMP responses to damage and cell death in kidney disease. J Am Soc Nephrol **22**:416–425. https://doi.org/10.1681/ASN.2010040430.
44. **Spruessel A, Steimann G, Jung M, Lee SA, Carr T, Fentz AK, Spangenberg J, Zornig C, Juhl HH, David KA.** 2004. Tissue ischemia time affects gene and protein expression patterns within minutes following surgical tumor excision. Biotechniques **36**:1030–1037. https://doi.org/10.2144/04366RR04.
45. **Stroo I, Stokman G, Teske GJD, Raven A, Butter LM, Florquin S, Leemans JC.** 2010. Chemokine expression in renal

ischemia/reperfusion injury is most profound during the reparative phase. Int Immunol **22**:433–442. https://doi.org/10.1093/intimm/dxq025.

46. **Terker AS, de Caestecker M.** 2020. Modeling human disease: A mouse model of acute kidney injury to chronic kidney disease progression after cardiac arrest. Kidney Int **97**:22–24. https://doi.org/10.1016/j.kint.2019.09.017.
47. **Thakar CV, Christianson A, Himmelfarb J, Leonard AC.** 2011. Acute kidney injury episodes and chronic kidney disease risk in diabetes mellitus. Clin J Am Soc Nephrol **6**:2567–2572. https://doi.org/10.2215/CJN.01120211.
48. **Timchalk C, Finco DR, Quast JF.** 1997. Evaluation of renal function in rhesus monkeys and comparison to beagle dogs following oral administration of the organic acid triclopyr (3,5,6-trichloro-2-pyridinyloxyacetic acid). Fundam Appl Toxicol **36**:47–53. https://doi.org/10.1006/faat.1996.2285.
49. **Tsutsumi Y.** 2021. Pitfalls and caveats in applying chromogenic immunostaining to histopathological diagnosis. Cells **10**:1501. https://doi.org/10.3390/cells10061501.
50. **Van Why SK, Mann AS, Ardito T, Siegel NJ, Kashgarian M.** 1994. Expression and molecular regulation of Na(+)-K(+)-ATPase after renal ischemia. Am J Physiol **267**:F75–F85. https://doi.org/10.1152/ajprenal.1994.267.1.F75.
51. **Vogetseder A, Picard N, Gaspert A, Walch M, Kaissling B, Le Hir M.** 2008. Proliferation capacity of the renal proximal tubule involves the bulk of differentiated epithelial cells. Am J Physiol Cell Physiol **294**:C22–C28. https://doi.org/10.1152/ajpcell.00227.2007.
52. **Waikar SS, Liu KD, Chertow GM.** 2008. Diagnosis, epidemiology and outcomes of acute kidney injury. Clin J Am Soc Nephrol **3**:844–861. https://doi.org/10.2215/CJN.05191107.
53. **Xie JX, Li X, Xie Z.** 2013. Regulation of renal function and structure by the signaling Na/K-ATPase. IUBMB Life **65**:991–998. https://doi.org/10.1002/iub.1229.
54. **Yu SM, Bonventre JV.** 2018. Acute kidney injury and progression of diabetic kidney disease. Adv Chronic Kidney Dis **25**:166–180. https://doi.org/10.1053/j.ackd.2017.12.005.
55. **Zhou B, Lu Y, Hajifathalian K, Bentham J, Di Cesare M, Danaei G, Bixby H, Cowan MJ.** 2016. Worldwide trends in diabetes since 1980: A pooled analysis of 751 population-based studies with 4·4 million participants. Lancet **387**:1513–1530. https://doi.org/10.1016/S0140-6736(16)00618-8.
56. **Zhou D, Fu H, Liu S, Zhang L, Xiao L, Bastacky SI, Liu Y.** 2019. Early activation of fibroblasts is required for kidney repair and regeneration after injury. FASEB J **33**:12576–12587. https://doi.org/10.1096/fj.201900651RR.
57. **Zhou J, Fan Y, Tang S, Wu H, Zhong J, Huang Z, Yang C, Chen H.** 2017. Inhibition of PTEN activity aggravates cisplatin-induced acute kidney injury. Oncotarget **8**:103154–103166. https://doi.org/10.18632/oncotarget.20790.